European Journal of Radiology Open 3 (2016) 230–235

European Journal of Radiology Open

journal homepage: www.elsevier.com/locate/ejro

Treatment response after radioembolisation in patients with hepatocellular carcinoma—An evaluation with dual energy computed-tomography

Jens Altenbernd*, Axel Wetter, Michael Forsting, Lale Umutlu

Institute of Diagnostic and Interventional Radiology and Neuroradiology, University Hospital Essen, Germany

ARTICLE INFO

Article history:
Received 22 June 2016
Received in revised form 7 August 2016
Accepted 9 August 2016
Available online 25 August 2016

Keywords:
Liver
Radioembolisation
Dual energy
CT staging

ABSTRACT

Purpose: The aim of this prospective study was to examine the diagnostic value of dual-energy CT (DECT) in the assessment of response of HCC after radioembolisation (RE).
Material and methods: 40 HCC patients with 82 measurable target lesions were included in this study. At baseline and follow-up examination target lesions were evaluated with (IU), AASLD and Choi measurement criteria. Disease control was defined as the sum of complete response (CR), partial response (PR), progression disease (PD) and stable disease (SD).
Results: With Choi and IU more patients were considered than PR and less than PD and SD. According to AASLD more patients were measured as SD and PD than PR. 26/40 patients were classified as PR with IU. In contrast measurements with AASLD in only 8/26 patients were also classified as PR. 6/12 SD patients measured with IU were measured as PD with AASLD. 4/26 patients classified with IU as PR were described as SD with CHOI, 10/14 SD patients measured with CHOI were SD according to IU, the other 4 patients were PR with IU. 2/4 PD patients according to CHOI were SD with IU.
Conclusion: More patients by IU were classified as SD versus PD and PR versus SD. We attribute this to the more detailed consideration of the HU differences between the virtual native and contrast-enhanced series generated by DECT. Iodine uptake (IU) in HCC measured and visualized with DECT is a promising imaging method for the assessment of treatment response after radioembolisations.
Key points: —dual energy CT of hypervascular tumors such as HCC allows to quantify contrast enhancement without native imaging.
—this can be used to evaluate the therapy response after Radioembolization.

1. Introduction

Selective internal radiation therapy (SIRT) with 90yttrium microspheres – also known as radioembolisation (RE)- is a rapidly evolving therapy option for inoperable HCC [1–6].

The response to treatment is assessed by critical clinical and laboratory parameters as well as by post- interventional cross-sectional imaging including CT or MRI. In addition to the changes in tumor size vascularization is an important marker for therapy monitoring [7–15].

In responders HCC lesions ideally show a reduction in size and decreased hyper-vascularity after RE. In some cases, a stable or even increased tumor size (so-called pseudo-progression) with reduced blood flow to the tumor mass is reported [16]. This may be attributed to tumor necrosis, hemorrhage and edema leading to increased tumor size.

Assessment of tumor response should incorporate the reduction in viable tumor burden, defined by the area (EASL) [17] or diameter (AASLD) [18] measurement of contrast enhancing tumor on arterial phase imaging to assess the tumor response. AASLD diameter measurement of viable tumor is used in clinic and considered as the standard assessment of treatment efficiency in patients receiving antiangiogenic therapy [19].

Choi et al. have proposed the measurement of CT density as a potential indicator of gastrointestinal stromal tumor (GIST) response in patients undergoing targeted therapy [20].

In rare cases, however, HCC response may result in increased density because of the intratumoral hemorrhage, which is a rare effect observed during sorafenib therapy [15], thus result mislead

* Corresponding author at: Institute of Diagnostic and Interventional Radiology and Neuroradiology, University Hospital Essen, Hufelandstr.55, 45122 Essen, Germany.
E-mail address: jens.altenbernd@gmail.com (J. Altenbernd).

http://dx.doi.org/10.1016/j.ejro.2016.08.002

tumor density measurements and failed Choi response assessement. Therefore, ideally, new parameter directly related with neovascularisation should be acquired to assess the density differences related to contrast medium accumulation, or, those related to vital and vascularized tumor tissue [7].

Dynamic contrast-enhanced CT perfusion has been explored as potential new method for assessing response of tumor vascularization to antiangiogenic therapy but in clinic practice it is prohibited regarding the limitations (e.g. limited coverage of all tumor sites, unstandardized postprocessing, radiation dose) [21].

A recent development in CT has been the introduction of dual energy technology [22]. On such CT systems, two X-ray tubes can be operated at different tube currents, making dual energy scanning feasible. Dual energy CT implies simultaneous acquisition of data sets at two different photon spectra in a single CT examination [23] resulting in the ability to reconstruct the data at 80-kVp, 140-kVp, and weighted-average. The weighted-average data set is a combination of image data from the 80- and 140-kVp data sets and can be used to generate a virtual 120-kVp data set. In addition, virtual non-enhanced data sets can be reconstructed by using post-processing algorithms [24,25].

One important advantage of dual energy CT (DECT) when compared with a single-source system is the option to use the two tubes at different tube currents offering differentiation of materials of non-equal density. The higher the difference in the two tube currents (e.g. 80 kVp and 140 kVp) used for imaging the better is the differentiation between two materials of different density [23]. Based on these advantages potential applications of dual energy CT when evaluating the abdomen are for example [26]: Quantification and visualization of contrast enhancement, reconstruction of virtual non-enhanced images from the existing data sets obviating the need for additional non-enhanced scans. Consequently, radiation exposure for the patient may be reduced. Furthermore, calcifications may be quantified and anatomical structures of high attenuation (such as the bone) can be removed semiautomatically.

DECT) allows selective quantification and visualization of iodine-related density differences and improves the ability to detect contrast agent and to distinguish high-density substances created by iodine from those created by hemorrhage [7,21].

The aim of this prospective study was to examine the diagnostic value of iodine uptake (IU) measured with dual-energy CT (DECT) for the assessment of therapy response after RE in patients with HCC compared to measurements based on AASLD and Choi. We hypothesize that DECT may help to determine the exact contrast uptake in tumors, which could represent an important response marker in addition to changes in size.

2. Material and methods

2.1. Patient population

We prospectively analyzed data of all HCC patients who received radioembolisation and monitoring by DECT in our institution between May 2009 and January 2010. Baseline contrast enhanced DECT scan was obtained three weeks before treatment and at least one follow-up scan was obtained 12 weeks after radioembolisation. If bilobar disease was present radioembolisation treatment was staged and follow-up scan was performed 12 weeks after the last treatment.

The inclusion criteria were:

- inoperable (due to size, localization) HCC; hepatic function Child–Pugh Class A or B; presence of a measurable target lesion showing intratumoral arterial enhancement in contrast enhanced DECT [27]. The measurable diameter was at least 1 cm and the lesion was suitable for repeated measurements;
- the exclusion criteria were: prior systemic treatment; contrast allergy; renal dysfunction; hypoenhancing tumor without wash out; prior transarterial chemoembolization (TACE), or radiofrequence ablation (RFA).

Table 1
Patient demographics.

Variable	Value
Age(Years)	
mean	66.2 + - 8.3
range	52–77
Gender	
Males	24
Females	16
Etiology of liver cirrhosis	
Ethanol abuse	16
HBV	12
HCV	10
NASH	2
Child-Pugh class	
A	16
B	24
Baseline AFP	
Mean (ng/ml)	438
Range	92–4583

AFP, α-fetoprotein; HBV, hepatits B virus; HCV, hepatitis C virus; NASH, nonalcoholis steatohepatitis.

85 HCC patients were examined in our institution with DECT in this period, including 60 patients treated with radioembolisation. Finally, 40 out of 60 patients (34 men and 26 women) with 82 measurable target lesions (median 2 lesions/patient, range 1–4) were analyzed.

20 out of 60 patients were excluded from analysis 4 patients with no measurable target lesion, 16 patients with prior systemic treatment/transarterial chemoembolisation (TACE)/radiofrequence ablation (RFA).

This study was approved by our institutional review board and all patients provided written informed consent prior to their participation. Patientsí characteristics are displayed in Table 1.

2.2. DECT protocol

All CT scans were performed on a dual-source multi– detector scanner (Somatom Definition^{TM} Dual Source; Siemens Medical Solutions, Forchheim, Germany).

Patients were positioned slightly off center to the left to ensure complete coverage of the liver by the smaller field of view of detector B.

After intravenous injection of a non-ionic contrast agent (1,5 ml per kilogram of body weight, Xenetix 300^{TM}, *Guerbet, Sulzbach, Germany,* mean body weight 73 + - 17 kg, mean contrats amount 103 + - 10 ml, flow rate 4 ml/s) via an automated dual-syringe power injector (Accutron CT-D, Medtron, Saarbrücken, Germany) scanning of the arterial phase (AP) during inspiratory breath-hold was started. All patients were scanned in cranio-caudal direction from the dome of the liver to the iliac crest.

The timing for the AP scan was determined using the care bolus technique (Siemens Healthcare, Forchheim, Germany), AP scanning was automatically started 7 s after the attenuation coefficient of abdominal aortic blood reached 120 HU. The portal venous phase (PVP) images were acquired 30 s after AP.

All AP and PVP images were obtained in the dual energy (DE) mode. The DE scan was acquired with a detector collimation of

Table 2
Evaluation criteria used in the assessment of target lesion response.

	AASLD	CHOI	IU
CR	No viable lesion	No viable lesions	No viable lesions
PR	≥30% decrease of diameter	≥10% decrease of diameter or ≥15% decrease in tumor density (HU)	≥10% decrease of diameter or ≥15% decrease in tumor iodine uptake (HU)
PD	≥20% increase of diameter	≥10% increase of diameter and no PR by tumor density (HU)	≥10% increase of diameter and no PR by tumor iodine uptake (HU)
SD	Neither sufficient decrease for PR nor PD	Neither sufficient decrease for PR nor PD	Neither sufficient decrease for PR nor PD

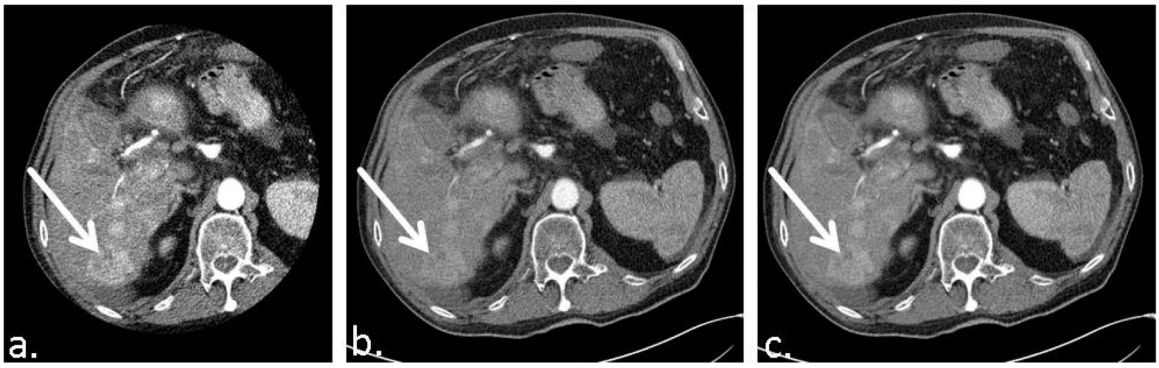

Fig. 1. The dual energy scanner generates three different series of images: 80-kVp images (a.), 140-kVp images (b.), and weighted-average images (c.).

14 × 1.2 mm on both detectors; slice thickness 3.0; rotation time, 0.5 s; pitch, 0.6; voltage tube A at 140 kVp and a reference value of 96 mAs and tube B at 80 kVp and a reference value of 404 mAs. For both tubes, an online dose modulation (Care DOSE 4D™, Siemens Medical Solutions) was used. For all scans, the gantry rotation speed was 0.5 s.

To calculate the mean iodine-uptake (IU) and density measurements of the tumor in the arterial contrast phase the dual energy software (Dual Energy™, Siemens Medical Solutions) was used. The contrast medium enhancement was quantified based on a three material decomposition assuming the main components fat, soft tissue and iodine. On the basis of calibration measurements performed by the manufacturer, the algorithm is able to transform spectral information of dual energy data into absolute values of iodine content. Additionally, the maximum transversal viable tumor diameter (according to AASLD criteria [18]) of each target lesion was measured properly in arterial phase CT images. Viable tumor was defined astumor tissue enhancing in arterial phase CE-DECT examinations after contrast medium injection [9,10].

DECT studies were evaluated retrospectively by two radiologists with more than 10 years of diagnostic experiences in a consensus mode. At baseline and follow-up examination target lesions were evaluated with AASLD and Choi measurement criteria (Table 2). AFP (α-fetoprotein) was measured before and 12 weeks after RE.

The response evaluation was performed on a per lesion basis; we did not take into consideration changes in non-target lesions, the appearance of new lesions nor change in extrahepatic tumor load.

Disease control was defined as the sum of complete response (CR), partial response (PR) and stable disease (SD). However, the objective response (OR) was defined as the sum of CR and PR, similar to other studies [14]. Unidimensional maximum transversal diameter of viable tumor was measured manually according to AASLD criteria [9,10]. Progressive disease (PD) refered to 20% increase, partial response (PR) to 30% decrease in diameter, complete response (CR) refered to complete disappearance of measurable lesions and stable disease (SD) is defined as a status between PD and PR. Tumor CT density was assessed using CT attenuation coefficients as described by Choi and colleagues in GIST [13]. PR according to Choi criteria was defined as a decrease in tumor density (measured in Hounsfield units, HU) of 15% or more on CT or a decrease in target size (largest diameter of target lesion, mm) of 10% or more.

2.3. Postprocessing and image reconstruction

Axial post-contrast images were reconstructed using a section thickness and an increment of 3 mm. The dual energy scanner generates three different series of images: 80-kV images, 140-kV images, and weighted-average images, which are based on attenuation information on scans obtained from both detectors, using 70% information from the high-kVp and 30% from the low-kVp scan (Fig. 1). Weighted-average images are similar to a 120-kVp scan of the abdomen and were used for measurements of contrast material uptake. Images were loaded onto a dedicated dual energy postprocessing workstation (syngo MMWP; Siemens Medical Solutions, Forchheim, Germany). Overlay images were reconstructed from the original data set by visualization of iodine. This calculation was based on a so-called three-material decomposition: Assuming that every voxel in the abdomen is composed of fat, soft tissue, and iodine, the algorithm generated a map that encodes the iodine distribution in each individual CT voxel. This map can subsequently be used to identify iodine in the image, resulting in an overlay image.

2.4. Qualitative analysis

Readers were asked to scroll through the sets of images on a dedicatd workstation (syngo MMWP, Siemens Medical Solutions) and to change window and/or level settings according to their personal preference. The greatest diameter and CT-attenuation of hypervascularized liver lesions in arterial phase in pre- and posttherpeutic DECT was measured. CT attenuation measurements were performed on axial images and adjusted manually.

2.5. Statistical analysis

Variables were expressed as mean ± standard deviation. Comparisons between groups were done with the λ2 test, the consistency evaluation with kappa statistical analysis an comparisons in groups were done using the one sample *t*-test and the correlations between different groups using Spearman correlation

Table 3
Response evaluation: comparison of evaluation criteria.

	CR	PR	PD	SD
AASLD	0	8/40	14/40	18/40
CHOI	0	22/40	4/40	14/40
IU	0	26/40	2/40	12/40

Table 4
Comparison of response evaluation results: AASLD vs. IU.

	IU					
AASLD		CR	PR	PD	SD	∑
	CR	0	0	0	0	0
	PR	0	8	0	0	8
	PD	0	6	2	6	14
	SD	0	12	0	6	18
	∑	0	26	2	12	

Table 5
Comparison of response evaluation results: CHOI vs. IU.

	IU					
CHOI		CR	PR	PD	SD	∑
	CR	0	0	0	0	0
	PR	0	22	0	0	22
	PD	0	0	2	2	4
	SD	0	4	0	10	14
	∑	0	26	2	12	

Table 6
Comparison of response evaluation results: AASLD vs. CHOI.

	CHOI					
AASLD		CR	PR	PD	SD	∑
	CR	0	0	0	0	0
	PR	0	8	0	0	8
	PD	0	4	4	6	14
	SD	0	10	0	8	18
	∑	0	22	4	14	

analysis. Significance was defined by $P < 0.05$. All statistical analyses were performed with the SPSS software package (version 21.0; SPSS, Inc., Chicago, Ill).

3. Results

The treatment response evaluated according to AASLD, Choi and IU is listed in Table 3. With Choi and IU more patients were considered as PR than as PD and SD. According to AASLD more patients were measured as SD and PD than as PR.

26/40 patients were classified as PR with IU. In contrast measurements with AASLD in only 8 of these 26 patients were also classified as PR, in 6/26 patients as PD and in 12/26 patients as SD. 6/12 SD patients measured with IU were measured as PD with AASLD, whereas 6/12 patients were classified SD with IU and AASLD (Table 4).

4/26 patients classified with IU as PR were described as SD with Choi, 10/14 SD patients measured with Choi were SD according to IU, the other 4 patients were PR with IU. 2/4 PD patients according to Choi were SD with IU (Table 5).

From 18 SD patients measured according to AASLD only 8/18 were SD based on Choi, but 10/18 PR with Choi. 6/14 SD patients with Choi were described as pD with AASLD (Table 6).

Table 7 illustrates significant changes of HU measured with Choi and IU and AFP measurements (ng/ml) from baseline to follow-up investigations. Between baseline and follow-up there were no significant differences of diameter-measurments according to AASLD.

Table 7
Response parameters at baseline and follow-up.

	Baseline	Follow-up	P value
AASLD (mm)	53.3 ± 23.4	50.2 ± 31.3	0.26
CHOI (HU)	56.6 ± 32.7	32.3 ± 21.8	<0.005
IU (HU)	34.2 ± 12.7	12.4 ± 9.3	<0.005
AFP (ng/ml)	438 ± 301	134 ± 73	<0.005

4. Discussion

The study examined the possibilities of DECT in the assessment of therapy response of hepatocellular carcinoma after radioembolization (RE).

In recent years, the importance of tumor perfusion in the assessment of response to therapy has more and more increased. Here, the changes in CT density values of the tumors as meaningful parameters were used in addition to size changes [8–15]. With the present study we now demonstrate that dual-energy CT can provide important information about the contrast uptake of hepatocellular carcinomas. Others studies showed that volumetric iodine uptake (VIU) is likely to be an optimized tumor response biomarker, first reflecting vital tumor burden in HCC [7]. The iodine uptake (IU) can also be quantified and visualized optically [21,28–31] (Figs. 2–4). The decisive advantage of DECT is that a native examination of the tumors before contrast injection to assess the iodine uptake is not necessary, because materials as iodine can be quantified using information of the different CT-tubes [32].

Our study has shown that the quantified iodine uptake of the tumors using DECT as an expression of tumor-perfusion is a promising parameter. In contrast to the absolute CT density value changes measured by Choi IU measurements with DECT led to changes in classifications of patients in tumor response after RE. Thus, we have shown that more patients by IU were classified as SD versus PD and PR versus SD. We attribute this to the more detailed consideration of the HU differences between the virtual native and contrast-enhanced series generated by DECT. Thus, therapy-induced necrosis was detected more precise with IU than by absolute density measurements according to Choi.

Account of tumor perfusion can decisive influence the assessment of treatment response as other studies could prove. For example, patients can be rated as PR, when a decrease in the sum of the lesion densities (HU) of ≥15% can be found, regardless of changes in tumor size [10].

Other studies showed that both VIU (volume iodine uptake) and Choi can reflect the iodinated contrast medium accumulation in the vital parts of tumor and thus can be used to evaluate the intratumoral blood and vascular changes. However, the mean tumor density of Choi reflects in their opinion not only the accumulation of iodine, but also the mixed internal materials of tumor, as vital tumor, necrosis tissue even hemorrhage caused by targeted therapies. Intratumoral hemorrhage could raise the tumor density and could mislead the evaluation of therapy response [7].

Our study has some limitations. First, only responses of target lesions were evaluated and the overall response of patients was not evaluated. Larger patient sampling and overall response of patient should be done in future studies.

Second, future studies should clarify how the iodine uptake correlates with histopathological changes under therapy. We have not made any histological examination.

Additionally, further quantitative studies should correlate IU with other independent tumor response parameters, such as overall survival, to define iodine-uptake thresholds more appropriate for the different response categories, and to evaluate the value of IU as a more independent tumor response parameter for monitoring of HCC targeted therapy.

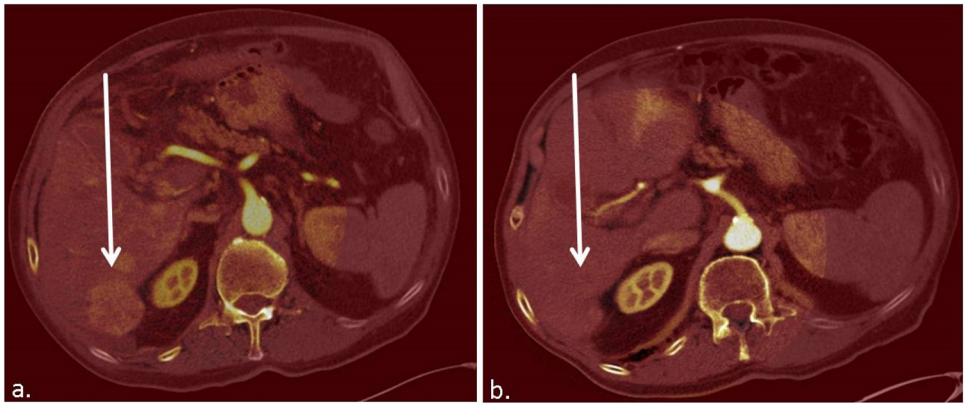

Fig. 2. HCC in segment 6 of the liver. Overlay images generated with DECT before (a.) and after RE (b.).

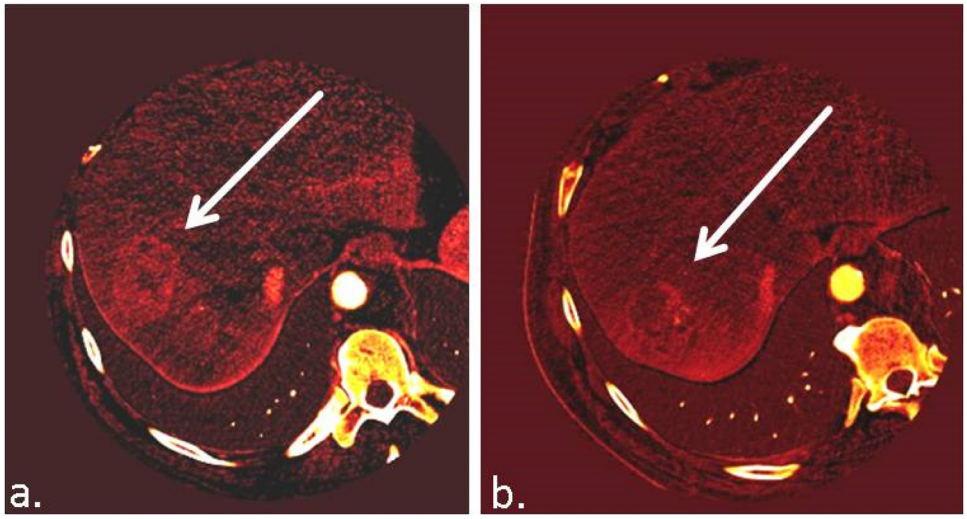

Fig. 3. HCC in segment 7/8 of the liver. Overlay images generated with DECT before (a.) and after RE (b.).

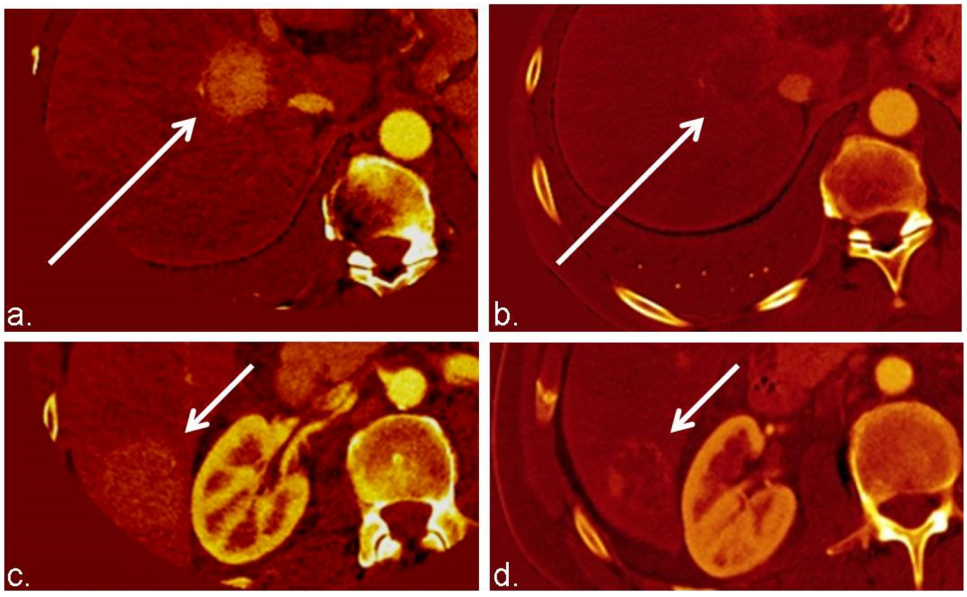

Fig. 4. HCC in segment 5 and 6 of the liver. Overlay images generated with DECT before (a.; c.) and after RE (b.; d.).

Conclusion: Iodine uptake (IU) in HCC measured and visualized with DECT is a promising imaging method for the assessment of treatment response after radioembolisations. As IU reflects vital tumor burden in HCC, it is likely to be an optimal tumor response biomarker in HCC.

4.1. Clinical relevance

1. Using the dual energy CT treatment monitoring can be done more precisely.
2. Contrast enhancement can be quantified without prior native images.
3. Patients benefit from a more accurate treatment monitoring and less radiation exposure.

Conflict of interest

None.

References

[1] J.C. Andrews, S.C. Walker, R.J. Ackermann, L.A. Cotton, W.D. Ensminger, B. Shapiro, Hepatic radioembolization with yttrium-90 containing glass microspheres: preliminary results and clinical follow-up, J. Nucl. Med. 35 (10) (1994) 1637–1644.
[2] G. Antoch, S.P. Mueller, M. Hamami, et al., Selective internal radiotherapy (SIRT) for hepatocellular carcinoma, RoFo 182 (8) (2010) 660–670.
[3] J.F. Geschwind, R. Salem, B.I. Carr, et al., Yttrium-90 microspheres for the treatment of hepatocellular carcinoma, Gastroenterology 127 (Suppl. (1)) (2004) S194–S205.
[4] P. Hilgard, S. Muller, M. Hamami, et al., Selective internal radiotherapy (radioembolization) and radiation therapy for HCC—current status and perspectives, Z. Gastroenterol. 47 (1) (2009) 37–54.
[5] S.M. Ibrahim, R.J. Lewandowski, R.K. Ryu, et al., Radiographic response to yttrium-90 radioembolization in anterior versus posterior liver segments, Cardiovasc. Intervent. Radiol. 31 (6) (2008) 1124–1132.
[6] R. Salem, R.J. Lewandowski, B. Atassi, et al., Treatment of unresectable hepatocellular carcinoma with use of 90Y microspheres (TheraSphere): safety, tumor response, and survival, J. Vasc. Intervent. Radiol. 16 (12) (2005) 1627–1639.
[7] X. Dai, H.P. Schlemmer, B. Schmidt, et al., Quantitative therapy response assessment by volumetric iodine-uptake measurement: initial experience in patients with advanced hepatocellular carcinoma treated with sorafenib, Eur. J. Radiol. 82 (2) (2013) 327–334.
[8] B. Atassi, A.K. Bangash, A. Bahrani, et al., Multimodality imaging following 90Y radioembolization: a comprehensive review and pictorial essay, Radiographics 28 (1) (2008) 81–99.
[9] L. Bester, P.G. Hobbins, S.C. Wang, R. Salem, Imaging characteristics following 90yttrium microsphere treatment for unresectable liver cancer, J. Med. Imaging Radiat. Oncol. 55 (2) (2011) 111–118.
[10] O. Dudeck, M. Zeile, P. Reichardt, D. Pink, Comparison of RECIST and Choi criteria for computed tomographic response evaluation in patients with advanced gastrointestinal stromal tumor treated with sunitinib, Ann. Oncol. 22 (8) (2011) 1828–1833.
[11] J. Edeline, E. Boucher, Y. Rolland, et al., Comparison of tumor response by Response Evaluation Criteria in Solid Tumors (RECIST) and modified RECIST in patients treated with sorafenib for hepatocellular carcinoma, Cancer 118 (1) (2012) 147–156.
[12] H.B. El-Serag, K.L. Rudolph, Hepatocellular carcinoma: epidemiology and molecular carcinogenesis, Gastroenterology 132 (7) (2007) 2557–2576.
[13] S. Faivre, M. Zappa, V. Vilgrain, et al., Changes in tumor density in patients with advanced hepatocellular carcinoma treated with sunitinib, Clin. Cancer Res. 17 (13) (2011) 4504–4512.
[14] E. Frampas, N. Lassau, M. Zappa, M.P. Vullierme, S. Koscielny, V. Vilgrain, Advanced hepatocellular carcinoma: early evaluation of response to targeted therapy and prognostic value of perfusion CT and dynamic contrast enhanced-ultrasound. Preliminary results, Eur. J. Radiol. 82 (5) (2013) e205–e211.
[15] T.F. Jakobs, R.T. Hoffmann, K. Tatsch, C. Trumm, M.F. Reiser, Therapy response of liver tumors after selective internal radiation therapy, Radiologe 48 (9) (2008) 839–849.
[16] M. Uhrig, M. Sedlmair, H.P. Schlemmer, J.C. Hassel, M. Ganten, Monitoring targeted therapy using dual-energy CT: semi-automatic RECIST plus supplementary functional information by quantifying iodine uptake of melanoma metastases, Cancer Imaging 13 (3) (2013) 306–313.
[17] J. Bruix, M. Sherman, J.M. Llovet, et al., Clinical management of hepatocellular carcinoma. Conclusions of the Barcelona-2000 EASL conference. European Association for the Study of the Liver, J. Hepatol. 35 (3) (2001) 421–430.
[18] R. Lencioni, J.M. Llovet, Modified R.E.C.I.S.T. (mRECIST) assessment for hepatocellular carcinoma, Semin. Liver Dis. 30 (1) (2010) 52–60.
[19] D. Spira, M. Fenchel, U.M. Lauer, et al., Comparison of different tumor response criteria in patients with hepatocellular carcinoma after systemic therapy with the multikinase inhibitor sorafenib, Acad. Radiol. 18 (1) (2011) 89–96.
[20] H. Choi, C. Charnsangavej, S.C. Faria, et al., Correlation of computed tomography and positron emission tomography in patients with metastatic gastrointestinal stromal tumor treated at a single institution with imatinib mesylate: proposal of new computed tomography response criteria, J. Clin. Oncol. 25 (13) (2007) 1753–1759.
[21] P. Apfaltrer, M. Meyer, C. Meier, et al., Contrast-enhanced dual-energy CT of gastrointestinal stromal tumors: is iodine-related attenuation a potential indicator of tumor response? Invest. Radiol. 47 (1) (2012) 65–70.
[22] T.G. Flohr, C.H. McCollough, H. Bruder, et al., First performance evaluation of a dual-source CT (DSCT) system, Eur. Radiol. 16 (2) (2006) 256–268.
[23] T.R. Johnson, B. Krauss, M. Sedlmair, et al., Material differentiation by dual energy CT: initial experience, Eur. Radiol. 17 (6) (2007) 1510–1517.
[24] H. Scheffel, P. Stolzmann, T. Frauenfelder, et al., Dual-energy contrast-enhanced computed tomography for the detection of urinary stone disease, Invest. Radiol. 42 (12) (2007) 823–829.
[25] T.C. Johnson, B. Krauß, M. Sedlmair, et al., Material differentiation by dual energy CT: initial experience, Eur. Radiol. 17 (6) (2007) 1510–1517.
[26] A. Graser, T.R. Johnson, H. Chandarana, M. Macari, Dual energy CT: preliminary observations and potential clinical applications in the abdomen, Eur. Radiol. 19 (1) (2009) 13–23.
[27] T. Kawaoka, H. Aikata, E. Murakami, et al., Evaluation of the mRECIST and alpha-fetoprotein ratio for stratification of the prognosis of advanced-hepatocellular-carcinoma patients treated with sorafenib, Oncology 83 (4) (2012) 192–200.
[28] C.L. Brown, R.P. Hartman, O.P. Dzyubak, et al., Dual-energy CT iodine overlay technique for characterization of renal masses as cyst or solid: a phantom feasibility study, Eur. Radiol. 19 (5) (2009) 1289–1295.
[29] A.J. Chu, J.M. Lee, Y.J. Lee, S.K. Moon, J.K. Han, B.I. Choi, Dual-source, dual-energy multidetector CT for the evaluation of pancreatic tumours, Br. J. Radiol. 85 (1018) (2012) e891–8.
[30] C.N. De Cecco, A. Darnell, M. Rengo, et al., Dual-energy CT: oncologic applications, AJR Am. J. Roentgenol. 199 (Suppl. (5)) (2012) S98–S105.
[31] T. Heye, R.C. Nelson, L.M. Ho, D. Marin, Boll DT. Dual-energy CT applications in the abdomen, AJR Am. J. Roentgenol. 199 (Suppl. (5)) (2012) S64–70.
[32] T.R. Johnson, Dual-energy CT general principles, AJR Am. J. Roentgenol. 199 (Suppl. (5)) (2012) S3–S8.